UNIVERSITAT DE BARCELONA

FERN–LIKE STRUCTURES IN THE WILD SET OF THE STANDARD AND SEMISTANDARD MAPS IN $\mathbb{C}^2$

by

Vasily G. Gelfreich, Vladimir F. Lazutkin,
Carles Simó and Michael B. Tabanov

AMS Subject Classification: 58F13

Mathematics Preprint Series No. 91
March 1991

FERN-LIKE STRUCTURES IN THE WILD SET OF THE STANDARD AND SEMISTANDARD MAPS IN C^2

by

Vasily G. Gelfreich *, *Vladimir F. Lazutkin* *,
Carles Simó **, *and Michael B. Tabanov* *

* Chair of Applied Mathematics of the Leningrad Institute of Aircraft Instrumentation Hertzen' st. 67, Leningrad 190000 USSR.

** Dept. de Matemàtica Aplicada i Anàlisi, Universitat de Barcelona, Gran Via 585, 08007 Barcelona, Spain.

Abstract. The standard and semistandard maps are considered in $\mathbb{C}^2$ and the behaviour of the iterates on complex invariant manifolds of them is studied. This is an attempt to understand complicated real dynamics by looking at the enlarged complex dynamics. Expansions of the manifolds are given as well as criteria for escaping points and hyperbolicity. Some numerical explorations suggest the presence of fractal structures of fern type. Several conjectures suggested by these preliminary explorations are stated.

§ 1. Introduction

One of the most interesting problems of dynamics is the study of the coexistence of regular and stochastic behaviour of the trajectories of a Hamiltonian System [A], [AKN], [LL], [MP], [M2]. Essentially the problem reduces to the study of the behaviour of the separatrices (stable, W^s, and unstable, W^u, manifolds) of periodic hyperbolic orbits. The homoclinic phenomena give rise to a very complicated pattern of the net created by W^s and W^u, as pointed out by Poincaré [P] many years ago. Nevertheless, little is known, up to now, about the structure of this net.

It seems natural to apply to this problem the principle of analytical continuation into the complex domain. What happens to the trajectories lying on the analytical continuations of W^u and W^s? The aim of this paper is to make the first step in that direction: to explore numerically simple models.

A good model to study the mentioned coexistence of random and regular motion in Hamiltonian systems with two degrees of freedom is the dynamical system generated by iterations of the standard map ([G], [C], [L1]), defined by

$$\begin{aligned} &SM(x,y) = (x_1, y_1), \\ &x_1 = x + y_1, \\ &y_1 = y + \varepsilon \sin x. \end{aligned} \tag{1.1}$$

Usually SM is considered as a map of the cylinder $(\mathbf{R}/2\pi\mathbf{Z}) \times \mathbf{R}$ into itself (one can also consider as a map in the 2–torus $(\mathbf{R}/2\pi\mathbf{Z})^2$). We prefer here to consider (1.1) as a map in $\mathbf{R}^2$, keeping in mind its commutativity with the shifts in the x and y directions by 2π.

Since $\sin x$ is an entire function (1.1) can be prolonged analytically to an analytic diffeomorphism in $\mathbf{C}^2$. We retain the same notation for the map, SM, and the variables (x,y). The SM preserves the area and the orientation. This is equivalent to the preservation of $dx \wedge dy$:

$$dx_1 \wedge dy_1 = dx \wedge dy. \tag{1.2}$$

This equation remains valid in $\mathbf{C}^2$. We will refer to an analytical map $(x,y) \to (x_1, y_1)$ satisfying (1.2) as an *analytical symplectic map.*

Let us change the variables (x,y) to the new ones (u,v) by means of

$$\begin{aligned} &x = -i \log \frac{\varepsilon}{2} + iu, \\ &y = iv. \end{aligned} \tag{1.3}$$

Then SM is written as $(u,v) \to (u_1,v_1)$ with

$$u_1 = u + v_1\,,$$
$$v_1 = v + e^u - \frac{\varepsilon^2}{4}\, e^{-u}\,. \tag{1.4}$$

If $Im\ x$ is positive and sufficiently large, the last term in the second line of (1.4) is small. We may consider it as a small perturbation when studying the motion of a point under the iterations of SM in that part of the complex phase space. The unperturbed map, known as the semistandard map (SSM), appears to be independent of ε and reads

$$SSM(u,v) = (u_1,v_1)\,,$$
$$u_1 = u + v_1\,, \tag{1.5}$$
$$v_1 = v + e^u\,.$$

This map was introduced (in a slightly different form) by Greene and Percival [GP] and has been studied by many authors ([Pe], [Ma], [LST]).

In the present paper we study numerically the global behaviour of the complex trajectories of SM and SSM belonging to the unstable separatrices (of the origin for SM and of "minus infinity" for SSM). We found that the points which go ultimately to the domain with "wild" hyperbolic features, form a pattern on a fundamental domain of W^u which reminds the leaves of a fern, in the case of SSM. For the SM some of the end points of the leaves reach the real line exactly at homoclinic points.

§ 2. Parametric representation for the unstable separatrix of SM

For positive values of the parameter ε, the origin (0,0) is a hyperbolic fixed point, the largest eigenvalue of the linear part of SM at this point being

$$\lambda = 1 + \frac{\varepsilon}{2} + \sqrt{\varepsilon + \varepsilon^2/4}\,. \tag{2.1}$$

By using Moser's Theorem ([M1] or [SM]), one can assert the existence of an analytical symplectic local diffeomorphism, Φ, defined in a complex neighbourhood, U, of (0,0) such that $\Phi(0,0) = (0,0)$ and it carries SM to the normal form:

$$\Phi \circ SM \circ \Phi^{-1} : (\xi,\eta) \longmapsto (\xi \cdot \Lambda(\xi\cdot\eta),\ \eta/\Lambda(\xi\cdot\eta))\,, \tag{2.2}$$

where Λ is an analytical function of one complex variable defined in a neighbourhood of 0 and satisfying $\Lambda(0) = \lambda$. Furthermore, by [FS], the neighbourhood U is independent of ε for $0 < \varepsilon < \varepsilon_0$, ε_0 fixed. The projections $\xi = pr_1\Phi$, $\eta = pr_2\Phi$ can be considered as (symplectic) coordinates in U: they are the *normal coordinates*.

Consider the complexified unstable manifold of the origin:

$$W^u = \left\{(x,y) \in \mathbf{C}^2 : SM^{-n}(x,y) \to (0,0) \quad \text{as} \quad n \to +\infty\right\} .$$

It follows from (2.2) that the subset of U defined by $\eta = 0$, denoted by W^u_{loc}, is contained in W^u, and

$$W^u = \bigcup_{n\geq 0} SM^n\left(W^u_{\text{loc}}\right) .$$

The coordinate ξ, being restricted to W^u_{loc}, can serve as a coordinate on W^u_{loc}. One can deduce from Moser's Theorem that this coordinate is defined uniquely up to a non zero constant multiplier. It is not difficult to obtain the parametric representation for W^u_{loc} :

$$\begin{aligned} &\xi \longmapsto W^u(\xi) = (x^u(\xi), y^u(\xi)) , \\ &x^u(\xi) = \sum_{k=1}^{\infty} \bar{a}_k \xi^k , \quad y^u(\xi) = \sum_{k=1}^{\infty} \bar{b}_k \xi^k . \end{aligned} \tag{2.3}$$

The map $SM_{\left|W^u_{\text{loc}}\right.}$ reads, in terms of ξ, as $\xi \longmapsto \lambda\xi$.

To obtain (2.3) is cheaper to look directly for the parametric representation instead of computing the normal form (see [S] for general comments). By using the fact that *sin* is an odd function we introduce

$$x^u = \sum_{n\geq 0} a_n \xi^{2n+1} , \quad y^u = \sum_{n\geq 0} b_n \xi^{2n+1} . \tag{2.4}$$

From the first line of (1.1) and the expression of $SM_{\left|W^u_{\text{loc}}\right.}$ in terms of ξ we get

$$a_n(\lambda^{2n+1} - 1) = b_n \lambda^{2n+1} . \tag{2.5}$$

Let us introduce two auxiliar series

$$\sum_{n\geq 0} c_n \xi^{2n} = \cos\left(\sum_{n\geq 0} a_n \xi^{2n+1}\right) , \quad \sum_{n\geq 0} d_n \xi^{2n+1} = \sin\left(\sum_{n\geq 0} a_n \xi^{2n+1}\right) . \tag{2.6}$$

From (2.6), by derivation and product, we obtain the recurrences

$$c_n = -\frac{1}{2n} \sum_{m+k=n-1} d_m\, a_k(2k+1)\,,$$

$$d_n = \frac{1}{2n+1} \sum_{m+k=n} c_m\, a_k(2k+1)\,, \tag{2.7}$$

started with $c_0 = 1$, $d_0 = a_0$.

From the second line of (1.1) we obtain

$$b_n\big(\lambda^{2n+1} - 1\big) = \varepsilon\, d_n\,. \tag{2.8}$$

As a_n is obtained from b_n by (2.5), that one from d_n by (2.8) and d_n in (2.7) contains a_n, we introduce $\bar{d}_n$, for $n \geq 1$, by

$$\bar{d}_n = \frac{1}{2n+1} \sum_{k=0}^{n-1} c_{n-k}\, a_k(2k+1)\,. \tag{2.9}$$

When $\bar{d}_n$ is available we compute d_n by

$$d_n = \bar{d}_n \left[1 - \frac{\varepsilon\, \lambda^{2n+1}}{(\lambda^{2n+1}-1)^2}\right]^{-1}\,. \tag{2.10}$$

If all the coefficients are known up to the index $n-1$ we compute successively c_n, $\bar{d}_n$, d_n, b_n and a_n by (2.7), (2.9), (2.10), (2.8) and (2.5). The normalization $a_0 = 4$ has been choosen. In this way we obtain the entire functions of (2.4).

We will also consider another coordinate z which parametrizes $W^u_{\rm loc}\backslash\{(0,0)\}$ and is linked with ξ by the formula

$$\xi = \mu\, \lambda^z\,, \tag{2.11}$$

where μ is a fixed positive constant. The map $SM_{\big|W^u_{\rm loc}}$ reads, in terms of z, as

$$z \longmapsto z + 1\,. \tag{2.12}$$

On the other hand, the values of z which differ by an integer times $(\log\, \lambda)^{-1} \cdot 2\pi\, i$ correspond to the same points of $W^u_{\rm loc}$. So, it is sufficient to look for the behaviour under the iterations of SM of the points with the values of z lying in the fundamental domain

$$0 \leq Re\, z < 1, \quad 0 \leq Im\, z < (\log\, \lambda)^{-1} \cdot 2\pi\,.$$

By using coordinates which are real in the real domain and taking into account the symmetry $(x,y) \longmapsto (-x,-y)$ we can reduce our study to one quarter of the fundamental domain, that is, to

$$\mathcal{D} = \left\{ 0 \le Re\, z < 1, \quad 0 \le Im\, z < \frac{\pi}{2 \log \lambda} \right\}. \tag{2.13}$$

Finally we can also parametrize one quater of the fundamental domain by setting

$$|\xi| = \mu \cdot \lambda^{\alpha}, \quad Arg\, \xi = \frac{\pi}{2} \beta. \tag{2.14}$$

Then, instead of $\mathcal{D}$ it is enough to consider the domain, independent of ε,

$$D = \{ 0 \le \alpha < 1, \quad 0 \le \beta < 1 \}. \tag{2.15}$$

The suitable value of μ should be selected according to λ (and, therefore, to ε) and the number of terms retained in (2.4).

§ 3. Parametric representation for the unstable separatix of SSM

The semistandard map SSM given by (1.5) does not possess a fixed point. Nevertheless, the minus infinity of $Re\, u$ can be considered in some sense as a fixed point. It was proven in [L1] that SSM has an invariant curve, Γ_-, which approximates, in the complex domain, the unstable separatrix W^u of SM if we change variables according to (1.3). The curve $\Gamma_-(x)$ can be represented parametrically as

$$x \longmapsto (u_-(x), v_-(x)),$$

where $u_-(x)$ and $v_-(x)$ are entire functions of the complex variable x, $v_-(x)$ satisfying the equation

$$v_-(x) = u_-(x) - u_-(x-1). \tag{3.1}$$

Then the parameter x goes to $x+1$ when we do one iteration of SSM.

It was also proven in [L1] that $u_-(x)$ admits the following asymptotic expansion

$$u_-(x) = -\log \frac{x^2}{2} + \sum_{k \ge 1} p_k\, x^{-2k}, \tag{3.2}$$

which is uniformly valid in a sector $\delta_0 \le Arg\, x \le 2\pi - \delta_0$, δ_0 fixed positive.

The coefficients p_k are obtained as follows. Let

$$u_-(x) = -\log\frac{x^2}{2} + w(x),\ w(x) = \sum_{n\geq 1} p_n\, x^{-2n}, \tag{3.3}$$

and δ^2 the second order centered difference operator

$$(\delta^2 u_-)(x) = u_-(x+1) - 2u_-(x) + u_-(x-1).$$

The invariance of Γ_- is equivalent to the equation

$$(\delta^2 u_-)(x) = \exp(u_-(x)). \tag{3.4}$$

From (3.4) and (3.3) we have

$$(\delta^2 w)(x) = \delta^2 \log\frac{x^2}{2} + \exp(u_-(x)) = \delta^2 \log\frac{x^2}{2} + \frac{2}{x^2}\exp(w(x)). \tag{3.5}$$

Let us introduce an auxiliar expansion by

$$\exp(w(x)) = \sum_{n\geq 0}\frac{q_n}{x^{2n}}, \tag{3.6}$$

giving, by derivation and product, the recurrence

$$q_n = \frac{1}{n}\sum_{k=0}^{n-1} q_k\, p_{n-k}(n-k), \quad q_0 = 1. \tag{3.7}$$

Using also the relations

$$\delta^2\frac{1}{x^{2n}} = 2\sum_{k\geq 1}\binom{-2n}{2k}x^{-(2k+2n)}, \tag{3.8}$$

$$\delta^2 \log\frac{x^2}{2} = 2\log\left(1-\frac{1}{x^2}\right) = -2\sum_{j\geq 1}\frac{1}{j}x^{-2j},$$

and substituting (3.6) and (3.8) in (3.5) we obtain

$$q_{m-1} = \frac{1}{m} + \sum_{n=1}^{m-1} p_n\binom{-2n}{2(m-n)}. \tag{3.9}$$

From (3.7) and (3.9) we isolate p_r, with $r = m-1$:

$$p_r = \frac{1}{2r^2+r-1}\left[\frac{1}{r}\sum_{k=1}^{r-1}(r-k)q_k\, p_{r-k} - \frac{1}{r+1} - \sum_{k=1}^{r-1} p_k\binom{-2k}{2(r+1-k)}\right]. \tag{3.10}$$

In (3.10) if $r = 1$ the summation sings run over an empty set, and $p_1 = -\frac{1}{4}$. Proceeding with (3.7) and (3.10) we obtain the desired coefficients.

The coefficients p_k increase quickly with k, like $\frac{(2k+1)!}{(2\pi)^{2k}}$, and q_k is very close to p_k. This is coherent with (3.7) and (3.10). In fact, if we define s_k by

$$p_k = (-1)^k \frac{(2k+1)!}{(2\pi)^{2k}} s_k \,, \tag{3.11}$$

then s_k seems to converge to 1.5034... when $k \to +\infty$.

We remark that the stable manifold of "minus infinity", $\Gamma_+(x)$ can be parametrized by

$$\Gamma_+(x) = (u_+(x), v_+(x)), \quad u_+(x) = u_-(-x),\ v_+(x) = -v_-(-x+1)\,. \tag{3.12}$$

§ 4. Escaping region to $-\infty$ for SSM

Consider the iteration of a point $(u, v) \in \mathbf{C}^2$ under the semistandard map

$$(u_n, v_n) = SSM^n(u, v), \quad n = 0, 1, 2, \ldots\,.$$

We say that (u, v) is *escaping to* $-\infty$ if there exists a finite $\lim_{n \to +\infty} v_n$ whose real part is negative. In this case the real part of u_n goes to $-\infty$, and the behaviour of the trajectories is quite regular.

If we restrict SSM to $\mathbf{R}^2$ the phase space is divided by the real portions of Γ_- and Γ_+ in three regions. To learn about the real behaviour of Γ_- and Γ_+ we need two lemmas.

Lemma 1. *For $Re\, u \to -\infty$, Γ_- and Γ_+ can be represented by graphs of functions, $v_- = g_-(u)$, $v_+ = g_+(u)$, respectively, of the type $g_\pm(u) = \sum_{j \geq 1} (\alpha_\pm)_j\, e^{ju/2}$.*

Proof: For shortness we skip the $\pm$ sign. Let $p = e^{u/2}$. In the (p, v) variables the SSM is given by

$$SSM : \begin{pmatrix} p \\ v \end{pmatrix} \longmapsto \begin{pmatrix} p_1 \\ v_1 \end{pmatrix} = \begin{pmatrix} p \exp\left(\frac{v+p^2}{2}\right) \\ v + p^2 \end{pmatrix}. \tag{4.1}$$

Let $g(u) = \sum_{j\geq 1} \alpha_j p^j$. Then the invariance is obtained by imposing

$$\sum_{j\geq 1} \alpha_j p^j + p^2 = \sum_{k\geq 1} \alpha_k p^k \exp\left(\frac{k}{2}\Big(\sum_{m\geq 1} \alpha_m p^m + p^2\Big)\right). \tag{4.2}$$

Let

$$\sum_{m\geq 0} \beta_{k,m} p^m = \exp\left(\frac{k}{2}\Big(\sum_{n\geq 1} \alpha_n p^n + p^2\Big)\right). \tag{4.3}$$

We introduce $\bar{\alpha}_j = \alpha_j + \delta_{j,2}$, where $\delta_{j,2} = 1$ if $j = 2$ and is zero otherwise. From (4.3) one has the recurrences

$$\beta_{1,m} = \frac{1}{2m} \sum_{n=1}^{m} \beta_{1,m-n}\, n\, \bar{\alpha}_n, \quad \text{for} \quad m \geq 1, \quad \beta_{1,0} = 1, \tag{4.4}$$

$$\beta_{k,m} = \frac{k}{m} \sum_{n=1}^{m} n\, \beta_{1,n}\, \beta_{k-1,m-n}, \quad \text{for} \quad m \geq 1, \quad \beta_{k,0} = 1.$$

Then, from (4.2) and (4.3) we have

$$\bar{\alpha}_j = \sum_{m=0}^{j-1} \beta_{j-m,m}\, \alpha_{j-m}. \tag{4.5}$$

However (4.4) and (4.5) define α_j, for $j \geq 1$, in an implicit way. We make it explicit as follows:

$$\alpha_1 = \pm\sqrt{2} \text{ (with sign + for } \Gamma_- \text{ and − for } \Gamma_+), \quad \beta_{1,0} = 1,\ \beta_{2,0} = 1,\ \beta_{1,1} = \frac{\alpha_1}{2},$$

$$\bar{\alpha}_2 = \frac{1}{2} \text{ (and then } \alpha_2 = -\frac{1}{2}),\ \beta_{3,0} = 1,\ \beta_{2,1} = \alpha_1,\ \beta_{1,2} = \frac{1}{2}, \quad \text{and, for} \quad j \geq 4$$

$$\beta_{j,0} = 1,\ \beta_{j-s,s} = \frac{j-s}{s} \sum_{n=1}^{s} n\, \beta_{1,n}\, \beta_{j-s-1,s-n}, \quad \text{for} \quad s = 1, \ldots, j-2, \tag{4.6}$$

$$\bar{\beta}_{1,j-1} = \frac{1}{2(j-1)} \sum_{n=1}^{j-2} \beta_{1,j-1-n}\, n\, \bar{\alpha}_n,$$

$$\alpha_{j-1} = -\frac{2}{j\alpha_1}\left[\sum_{n=2}^{j-2} \beta_{j-n,n}\, \alpha_{j-n} + \alpha_1\, \bar{\beta}_{1,j-1}\right],\ \beta_{1,j-1} = \bar{\beta}_{1,j-1} + \frac{1}{2}\alpha_{j-1}. \qquad \blacksquare$$

In fact it turns out that $\alpha_j = 0$ for all $j > 2$ even, and that all α_j, j odd, contain α_1 as a factor, the coefficient of α_1 in α_j, j odd, being the same for Γ_+ and Γ_-.

Lemma 2. *Let Γ_+ (resp. Γ_-) restricted to the real component, be given by the graph of a function $g_+(u)$ (resp. $g_-(u)$). Then $g'_+(u) < 0$, $g''_+(u) < 0$ for all u and both g'_+ and g''_+ behave like $-e^u$ for $u \to +\infty$ (resp. $g'_-(u) > 0$, $g''_-(u) > 0$ for all u and $g'_-(u) \sim 1 - u^{-1}$, $g''_-(u) \sim u^{-2}$ for $u \to +\infty$).*

Proof: From $T^{-1}\begin{pmatrix} u \\ g_+(u) \end{pmatrix} = \begin{pmatrix} u - g_+(u) \\ g_+(u) - \exp(u - g_+(u)) \end{pmatrix} = \begin{pmatrix} u_{-1} \\ v_{-1} \end{pmatrix}$ we obtain

$$(4.7)\quad \frac{dv_{-1}}{du_{-1}} = \frac{g'_+(u)}{1 - g'_+(u)} - \exp(u - g_+(u)),\ \frac{d^2v_{-1}}{du_{-1}^2} = \frac{g''_+(u)}{(1 - g'_+(u))^3} - \exp(u - g_+(u)).$$

As the assertion of the lemma is true in a fundamental domain for $u < 0$, $|u|$ large enough, as a consequence of Lemma 1, from (4.7) we obtain $g'_+ < 0$, $g''_+ < 0$ by induction. The limit behaviour follows immediately. The assertions for Γ_- are proved in a similar way. ∎

If we restrict to real behaviour the points below Γ_+ escape to $u = -\infty$ with a finite value of $v < 0$. Those points, under iterations of SSM^{-1} escape to $u = +\infty$ with $v \sim -e^u$. The points above Γ_- escape, under SSM, to $u = +\infty$ with $v \sim u$, and, under SSM^{-1}, to $u = -\infty$ with $v > 0$ finite. Finally, the points between Γ_- and Γ_+ escape to $u = +\infty$ both under SSM and SSM^{-1}, approaching Γ_- or Γ_+, respectively. However, during the iterations they can reach points close to the u axis with $u < 0$. As v is always increasing it seems that $SSM_{|\mathbb{R}^2}$ has a real analytical integral everywhere. Positive (resp. negative) iterates of the u axis give Γ_- (resp. Γ_+). For $u \to -\infty$ the behaviour of $\Gamma_\pm$ is given by Lemma 1. For $u \to +\infty$ one has $v \sim u - \log u + \frac{2 \log u}{u} - \frac{\log(\log u)}{u} + \dots$ for Γ_- and $v \sim -e^u - u + \log u + \dots$ for Γ_+.

It is useful to find explicitely a domain in $\mathbf{C}^2$ such that all the points in it are escaping to $-\infty$. We call such a domain a *swallowing domain.*

Lemma 3. *If the projection of (u,v) on $\mathbf{R}^2$ is below Γ_+ then (u,v) belongs to a swallowing domain.*

Proof: Let $u = a + bi$, $v = c + di$, $u_1 = a_1 + b_1 i$, $v_1 = c_1 + d_1 i$. Then $a_1 = a + c + e^a \cos b$, $c_1 = c + e^a \cos b$. The passage from (a,c) to (a_1,c_1) consists of two motions. One of them, $(a,c) \to (a + c, c)$, is a translation to the left. The other is simply to add $e^a \cos b \binom{1}{1}$. But this is bounded for the case $b = 0$, corresponding to real motion. Using Lemma 2 the conclusion follows. ∎

If $Re\, u$ is negative enough one can use Lemma 1 to obtain a swallowing domain. For $Re\, u$ positive large it is better the next criterion.

Lemma 4. *The domain Ω_g defined by the inequality*

$$Re\, v < g(Re\, u),$$

where

$$g(x) = -\log\left(1 + \frac{1}{2}e^x + \sqrt{\frac{1}{4}e^{2x} + e^x}\right) - \left(\frac{1}{2}\, e^x + \sqrt{\frac{1}{4}e^{2x} + e^x}\right), \tag{4.8}$$

is swallowing.

Proof: The set Ω_g can be represented as the union $\Omega_g = \bigcup_{K>0} \Omega_K$, where, given a positive value of K, the domain Ω_K is defined by the inequality

$$Re\, v < -f_K(Re\, u), \quad f_K(x) = K + \frac{e^{K+x}}{e^K - 1}.$$

Indeed, $g(x)$, is the envelop of the family $\{-f_K\}$. On the other hand, each Ω_K is swallowing. To prove this let us note that:

(i) Ω_K is invariant, i.e. $SSM(\Omega_K) \subset \Omega_K$. Using the notation of the proof of Lemma 3 for the real and imaginary parts of u, v, u_1, v_1, this follows from

$$K + c_1 = K + c + e^a \cos b < -\frac{e^{K+a}}{e^K - 1} + e^a \cos b = -\frac{e^{K+a}(1 - \cos b) + e^a \cos b}{e^K - 1}$$
$$\leq -\frac{e^a}{e^K - 1} < -\frac{\exp(a + K + c + e^a \cos b)}{e^K - 1} = -\frac{e^{K+a}}{e^K - 1},$$

because $K + c + e^a \cos b < -\dfrac{e^a}{e^K - 1} < 0$.

(ii) $Re\, v < -K$ for all $(u, v) \in \Omega_K$.

We have, using (1.5),

$$Re\, u_n \leq Re\, u - n\, K, \quad \text{and} \quad |v_{n+1} - v_n| \leq e^{-n\, K}.$$

The last inequality ensures the existence of $\lim_{n \to +\infty} v_n$, with the real part less than or equal to $-K$. ∎

We remark that, for real u, $g_+(u)$, as given in Lemma 1, approaches very well Γ_+ for $u < -5$, with a relative error less than 10^{-16}. On the other hand g, as given by Lemma 4, approaches very well Γ_+ for $u > 30$. For $u = 0$ a direct numerical computation gives for Γ_+ the value -2.0441929... . Using g_+ and g we obtain -2.0598158... and -2.5804576... , respectively.

§ 5. Hyperbolicity

There is another type of behaviour of the trajectories $z_n = (u_n, v_n)$ of SSM which are characterized by the property $Re\, u_n \to +\infty$ as $n \to +\infty$, or, at least, $Re\, u_n \geq K$ for all $n \geq n_0$, K being positive sufficienty large. Such trajectories posses hyperbolic features. The same is true for the trajectories of SM having the property $Im\, x \to +\infty$ (or $-\infty$) as $n \to +\infty$.

More precisely, the statement about hyperbolicity can be expressed as follows.

Lemma 5. *(Existence of a contracting direction).*

Let $z_n = (u_n, v_n)$, $n \geq n_0$ be a semitrajectory of SSM such that

$$Re\, u_n \geq K > \log\,(2 + \sqrt{5})$$

for all $n \geq n_0$. Then there exists a nonzero vector ζ such that

$$\|T_{z_{n_0}} SSM^m \zeta\| \leq \lambda^m \|\zeta\|\,,$$

where

$$\lambda = \frac{\sqrt{5}}{e^K - 2} < 1\,.$$

Here $\|\cdot\|$ is the usual Euclidean norm in $\mathbf{C}^2$: $\|\zeta\|^2 = |\xi|^2 + |\eta|^2$ when $\zeta = (\xi, \eta)^T$.

Proof: It follows from (1.5) that the tangent $T_z SSM$ at $z = (u, v)$ is given by the matrix

$$\begin{pmatrix} 1 + e^u & 1 \\ e^u & 1 \end{pmatrix}.$$

Denote its inverse at a point $z_n = (u_n, v_n)$ by

$$M_n = \begin{pmatrix} 1 & -1 \\ -e^{u_n} & 1 + e^{u_n} \end{pmatrix}.$$

Consider the cone $\mathcal{K} \subset \mathbf{C}^2$ defined by the inequality $|\xi| \leq \frac{1}{2}|\eta|$ for $\zeta = (\xi, \eta)^T \in \mathbf{C}^2$. Applying M_n the cone $\mathcal{K}$ remains invariant provided $Re\, u_n \geq K \geq \log 4$. Indeed, if $(\xi, \eta)^T \in \mathcal{K}$, then $|\xi| \leq \frac{1}{2}|\eta|$, and $(\xi', \eta')^T = M_n (\xi, \eta)^T$ satisfies the relations

$$\begin{aligned} &\xi' = \xi - \eta, \quad \eta' = -e^{u_n}\xi' + \eta\,, \\ &|\eta| = |\xi' - \xi| \leq |\xi'| + \frac{1}{2}|\eta|, \quad |\eta| \leq 2|\xi'|, \\ &|\eta'| \geq e^K |\xi'| - |\eta| \geq (e^K - 2)|\xi'| \geq 2|\xi'|\,. \end{aligned}$$

Also M_n stretches the vectors belonging to $\mathcal{K}$

$$\|M_n\zeta\| \geq |\eta'| \geq e^K|\xi'| - |\eta| \geq \left(\frac{1}{2}\, e^K - 1\right)|\eta|\,.$$

Since $\|\zeta\| = \|(\xi,\eta)^T\| \leq \dfrac{\sqrt{5}}{2}\,|\eta|$ for $(\xi,\eta)^T \in \mathcal{K}$, we have

$$\|M_n\zeta\| \geq \lambda^{-1}\|\zeta\|\,.$$

It follows that the sequence

$$M_{n_0}\, M_{n_0+1} \ldots M_{n_0+m}\, \mathcal{K} \subset \mathcal{K}$$

converges to a nontrivial closed cone (in fact a line). The vectors of this line satisfy the thesis of the Lemma 5. ∎

Remark 1. It follows from the preservation of $du \wedge dv$ that SSM stretches other directions different from the one of Lemma 5. In particular, we obtain the mentioned uniqueness of this direction. (The intersection of the cones $M_{n_0}M_{n_0+1}\ldots M_n(\mathcal{K})$ for all $n \geq n_0$ is a line).

Remark 2. The same proof goes for SM represented in the from (1.4). One has to replace the condition $Re\, u_n \geq K > \log(2+\sqrt{5})$ by the more complicated one

$$\left|e^{u_n} + \frac{\epsilon^2}{4}e^{-u_n}\right| \geq e^K\,, \quad K > \log(2+\sqrt{5})\,,$$

for all $n \geq n_0$.

§ 6. Numerical explorations

Several explorations have been done concerning the behaviour of points on the unstable manifold (of the origin for SM and of minus infinity for SSM). We describe the procedures and summarize the results. First we present them for the semistandard map.

Using (3.2) a fundamental domain in the plane of the parameter x is an strip of the form $x_0 \leq Re\, x \leq x_0 + 1 < 0$. We looked first for a value of x_0 such that the minimum term in the sequence $\left\{|p_{k+1}(x_0+1)^{-2k-2}|\right\}$ be less than 10^{-20}. From (3.11), for a fixed k the minimum of $|p_{k+1}x^{-2k-2}|$ is attained for $|x| = ((2k+2)(2k+3))^{1/2}/2\pi$, and the

value of the minimum is, roughly, $1.5034\frac{(2k+3)!}{((2k+2)(2k+3))^{k+1}}$. This is less than 10^{-20} for $k \geq 26$, and we can use $x < -8.6736$. In all the computations with the SSM we shall use $x_0 = -10$ and the sum in (3.2) up to $n_0 = 26$. The relation $SSM(\Gamma_-(x)) = \Gamma_-(x+1)$ is satisfied for all the points tested except for the rounding errors (in double precision).

Given a point $\Gamma_-(x)$, with x in the strip, one computes successively iterates up to a maximum of N. If some of them is in swallowing domain, then the iteration is stopped. To this end Lemma 1 and Lemma 4 are used. If for the n–th iterate one has $Re\, u_n > M$, with M positive big, one considers that the point has entered the wild or hyperbolic set and the point is marked as a dot in the x strip. Of course, it is possible (almost sure) that the point will return to the finite part or to a swallowing domain after further iterates, but this has been the cutting criterion in our computations. If after N iterates the point does not enter the wild nor the swallowing region, then the computation is stopped for the orbit of this point. In most of the cases it turns out, looking to the orbit, that the point escapes to $-\infty$ very slowly, requiring a big number of iterates before reaching the swallowing domain given by Lemma 1. One topic for further research is to use energy–time canonical variables, as in [L2], to speed up the process.

The figure 1 displays the wild set in the x plane for $-10 < Re\, x \leq -9, |Im\, x| < 3$. Due to the symmetry it is enough to consider one half strip, and we have chosen $Im\, x \leq 0$. It becomes apparent that the figure is self similar, except in what concerns the narrow black region going down. It seems that this region extends to $Im\, x \to -\infty$. For values of $Im\, x$ less than -2 it becomes so narrow that it can be fitted by a curve. The temptative value

$$Re\, x = -10 + 3/4 - \sqrt{8}\, \exp(\sqrt{8}\, Im\, x) \tag{6.1}$$

is proposed. Several tests have been done using (6.1) and we have found an escape towards big values of $Re\, u$ for all of them. One difficulty is that during the iterations the points go to $Re\, u < 0$ (reaching a minimum value of $Re\, u \sim 2\pi Im\, x + 7.02$) and the number of iterates before reaching $Re\, u > M$ becomes very large (close to $0.1328 \exp(-\pi\, Im\, x)$). We remark that to use $M = 500$ or $M = e^{500}$ requires, only, one extra iteration. For starting points given by (6.1) the final values of $Im\, u$ and $Im\, v$ tend to -2π and 0, respectively.

The figures 2 to 9 contain various enlargements of fig. 1. The self similarity becomes more apparent and fern–like structures are clear, specially in figures 4 to 8. The figure 10 contains a big horizontal magnification of a part of the black narrow region that seems to lie around the curve given by (6.1).

We can also describe the behaviour of the orbits corresponding to black points in the preceeding figures. To this end it is only necessary to describe the behaviour of $\{u_n\}$,

(1.5) giving $v_n = u_n - u_{n-1}$. If $Im\, u \in \left(\frac{2k-1}{2}\pi, \frac{2k+1}{2}\pi\right]$ we say that the code of u is k. Then we can consider the itinerary as the sequence of codes of the successive points in the orbit. For instance, any real orbit in Γ_- has itinerary with all the entries equal to zero. The branch of the wild region going down to minus infinity in fig. 1 has itinerary 0^∞, -1, $(-2)^\infty$. We give some itineraries which show the pattern of formation. The tip of fig. 6 has itinerary $0^\infty, -1, -4$, $s = -2$, where $s = j$ means that from -4 on the step is -2, that is, we get $-6, -8, -10, \ldots$. The tips of the principal leaves in fig. 7 (the central one being magnified in fig. 8) have itineraries (from top to bottom) $0^\infty, -1, -4$, $s = -2$, $-42, -45, -47, -49, -52$, $s = -2$; $0^\infty, -1, -4$, $s = -2$, $-44, -47, -49, -51, -54$, $s = -2$; $0^\infty, -1, -4$, $s = -2$, $-46, -49, -51, -53, -56$, $s = -2$, respectively. Those leaves are secondary ones in the full picture. The itinerary of points in a tertiary leave, such as the one appearing to the right lower part in fig. 8 has another pattern. For this point we found $0^\infty, -1, -4$, $s = -2, -42, -45, -47, -49, -51, -54$, $s = -2, -92, -95, -97, -99, -102$, $s = -2$. The tip of the branch which appears to the right upper part in fig. 2 is $0^\infty, -1, -6$, $s = -4$.

On the other hand it seems that the dynamics of the SSM should be influenced by the one of exp. Going from exp to SSM we move from $\Delta u = \exp(u)$ to $\delta^2 u = \exp(u)$, Δ being the forward finite difference. Some results for exp can be found in [DK], [DT], [V]. We skip some conjectures concerning the behaviour of SSM to the final discussion.

For SM we use (2.4) with the parameters of (2.14). One can take higher order in (2.4) to be able to use $|\xi|$ relatively large and avoid initial iterates. This is quite convenient if ϵ is small. Now there is no swallowing region and the stopping criterion is to reach $|Im\, x_n| > M$ for some M big. The points start in $Im\, x > 0$ and they are classified according to the number of times that they jump from $Im\, x > 0$ to $Im\, x < 0$ or viceversa, before stopping.

The figures 11 to 14 have been obtained for $\epsilon = 0.5$. Figure 11 shows the points (in the ξ domain, represented by the parameters α and β) that reach $|Im\ x| > M$ with 0 jumps, that is, they escape to $Im\, x > M$. One can see a central part which tends to the real axis in fig. 11. It goes to a real homoclinic point. If in one fundamental domain of the real part of W^u we look at the two main homoclinic points (the ones with all the iterates on $0 < x < 2\pi$) we define the principal homoclinic point as the one which has one iterate on $x = \pi$, the other being denoted as secondary. The limit point on the central branch of fig. 11 is the secondary homoclinic. The figures 13 and 14 show a magnification of fig. 11 around the secondary homoclinic point by factors of 10^2 and 10^4, respectively. Again the fern like structures become apparent. The figure 12 shows the points escaping after 1

jump. The limit on the real axis of the branch going downwards close to the right border of the figure is the principal homoclinic point, and the magnifications look like figures 13 and 14.

Finally, the figures 15 and 16 correspond to $\epsilon = 0.1$. They give the points escaping after 1 jump and a magnification by a factor 10^4 of the lower limit of the central branch, respectively.

Beyond different scaling patterns we can ask for another difference when reducing ϵ. Such a decrease in ϵ produces the dissappearition of real homoclinic points by means of tangential homoclinic points. To study numerically the behaviour of them one should not use small ϵ because, due to the exponentially small size of the distances between the manifolds (see [L1] and [FS]), the simulations should be done with very high precision routines. Instead we take ϵ rather big. Going down with ϵ, two homoclinic points dissappear close to 1.31903953 and they move to the complex plane. Table I displays some values close to this homoclinic tangency. Hence, it seems that when ϵ increases, many tips of leaves of the fern-like structure for the SM move towards the real axis.

μ	*values of α for homoclinics*	μ	*values of α and β for homoclinics*
10000	0.277030527, 0.283242278	3950	0.280191408 ± i 0.000058952
9000	0.277308070, 0.282982918	3940	0.280191499 ± i 0.000105855
8000	0.277613833, 0.282695339	3920	0.280191681 ± i 0.000163294
7000	0.277959179, 0.282368176	3900	0.280191863 ± i 0.000205243
6000	0.278366075, 0.281979463	3000	0.280200046 ± i 0.000858965
5000	0.278890192, 0.281473531	2000	0.280209138 ± i 0.001229161
4000	0.279921479, 0.280460428	1000	0.280218231 ± i 0.001511248
3980	0.279989393, 0.280392877	0	0.280227273 ± i 0.001748406
3960	0.280097598, 0.280285037		
3955	0.280163005, 0.280219721		

Table I. Here $\mu = 10^8(\epsilon - 1.319)$.

§ 7. Discussion

It turns out that the behaviour of the standard and semistandard maps in $\mathbf{C}^2$, on some of their unstable separatrices, is extremely rich, with zones of regular motion and others of wild character. Furthermore the wild set seems to be, partially, self similar. We hope that the understanding of some properties of this complex map will clarify the real behaviour. We rise some questions.

a) Concerning SSM:

1) The wild set (black set in fig. 1) has zero measure if the cutting value M tends to $+\infty$.

2) All the structures, except the central one, have branches, of all the levels, which end at a finite point. Which one is the meaning of this point?

3) The central branch goes to $Im\, x \to -\infty$ with the asymptotic behaviour given by (6.1). Then it divides the fundamental domain or, equivalenty, if it belongs to a line γ with imaginary part going from $-\infty$ to 0, then the region between γ and $\gamma + 1 = T_1\gamma$ (the shift of γ by 1 real unit) is a fundamental domain.

4) Let $\mathcal{F}_0$ be the set of points in the fundamental domain between γ and $\gamma+1$ (as in 3)) not belonging to the wild set. Then the Fatou set is

$$\mathcal{F} \cup \bar{\mathcal{F}}, \quad \text{where} \quad \mathcal{F} = \bigcup_{n \in \mathbb{Z}} \mathcal{F}_n,\ \mathcal{F}_n = T_1^n \mathcal{F}_0 .$$

and $\bar{\mathcal{F}}$ denotes the complex conjugate of $\mathcal{F}$.

Furthermore let

$$v_\infty(x) = pr_2 \lim_{n \to +\infty} SSM^n \Gamma_-(x) .$$

Then v_∞ maps $\mathcal{F}_0$ into the left halfplane ($Re(v_\infty(x)) < 0$). When we approach the tip of one of the branches of the wild set, while remaining in $\mathcal{F}_0$, the image $v_\infty(x)$ goes to a rational multiple of 2π in the imaginary axis.

5) Inside each one of the branches there is a filament (a hair as in the case of the iteration of the complex exponential map) going to infinity. This filament is associated to some definite symbolic dynamics.

b) Concerning SM :

1) The fraction of points escaping after j jumps, with j fixed, goes to zero when M goes to $+\infty$.

2) The tips of the branches which go to the real axis are homoclinic points. They are dense on the real part of the domain of the variable ξ.

3) The tips of branches not reaching the real axis are complex homoclinic points. When an homoclinic (real) tangency is produced, for varying values of ε, and the homoclinic point dissappears, it becomes complex homoclinic.

Acknowledgements. The authors thank D. F. Escande, Y. Elskens and A. Verga for their help and the interest shown in the initial computations. V. F. L. thanks also A. Douady for the interest shown in the fractal structures, and the Centre de Recerca Matemàtica and the Universitat of Barcelona for finantial support making possible a visit to Barcelona. M. B. T. thanks the Université of Provence for finantial support in a visit to Marseille. C. S. thanks the support from Grant PB86–527 of CICYT and the computer facilities obtained from CIRIT.

References

[A] V. I. Arnold, "Mathematical methods of classical mechanics", Springer, Heidelberg, 1978.

[AKN] V. I. Arnold, V. V. Kozlov, A. I. Neishtadt, "Encyclopaedia of Mathematical Sciences", Vol. 3, Springer, Heidelberg, 1988.

[C] B. V. Chirikov, A universal instability of many–dimensional oscillator systems, Physics Reports **52** (1979), 263–379.

[DK] R. L. Devaney, M. Krych, Dynamics of EXP., Ergod. Th. & Dynam. Sys. **4** (1984), 35–82.

[DT] R. L. Devaney, F. Tangerman, Dynamics of entire functions near the essential singularity, preprint Boston University.

[FS] E. Fontich, C. Simó, The splitting of separatrices for analytic diffeomorphisms, Ergod. Th. & Dynam. Sys. **10**, 295–318.

[G] J. M. Greene, A method for determining a stochastic transition, J. Math. Phys. **20** (1979), 1183–1201.

[GP] J. M. Greene, I. C. Percival, Hamiltonian maps in the complex plane, Physica **3** D (1981), 530–548.

[L1] V. F. Lazutkin, Splitting of separatrices for the Chirikov's standard map, preprint (in russian), VINITI 6372/84.

[L2] V. F. Lazutkin, Analytical integrals of the semistandard map and the splitting of separatrices, (in russian), Algebra and Analysis **1** (1989), 116–131.

[LST] V. F. Lazutkin, I. G. Schachmanski, M. B. Tabanov, Splitting of separatrices for standard and semistandard mappings, Physica **40** D (1989), 235–248.

[LL] A. J. Lichtenberg, M. A. Lieberman, "Regular and stochastic Motion", Springer, Heidelberg, 1983.

[Ma] S. Marmi, Critical functions for complex analytic maps, J. of Physics A, to appear, 1990.

[MP] P. R. Meggar, I. C. Percival, The transition to chaos for a special solution of the area–preserving quadratic map, Physica **14** D (1984), 49–66.

[M1] J. Moser, The analytical invariants of an area preserving mapping near a hyperbolic fixed point, Comm. Pure App. Math. **9** (1956), 673–692.

[M2] J. Moser, Lectures on Hamiltonian Systems, Memoirs Amer. Math. Soc. **81** (1968), 1–60.

[Pe] I. C. Percival, Chaotic boundary of a Hamiltonian map, Physica **6** D (1982), 67–74.

[P] M. Poincaré, "Les méthodes nouvelles de la mécanique céleste", Vol. 1–3, Paris, Gauthier Villars, 1892, 1893, 1899.

[SM] C. Siegel, J. Moser, "Lectures on Celestial Mechanics", Springer, Heidelberg, 1971.

[S] C. Simó, On the analytical and numerical computation of invariant manifols, to appear in "Méthodes modernes de la mécanique céleste", Ed. D. Benest, C. Froeschlé.

[V] M. Viana da Silva, The differentiability of the hairs of exp(Z), Proceed. Amer, Math. Soc. **103** (1988), 1179–1184.

Captions for the figures

Figure 1.

Wild set for the SSM. Order of the expansion (3.2) : $n_0 = 26$. Cutting criterion : $M = 700$. Maximum number of iterates : $N = 20000$. Domain of x for Γ_- : $Re\, x \in (-10, -9]$, $Im\, x \in (-3, 0]$. Points in the grid: 480 × 1440. The domain magnified in figure 2 is shown.

Figure 2.

Magnification of figure 1. Domain of x for Γ_- : $Re\, x \in (-10 + 0.8, -10 + 1.0]$, $Im\, x \in (-0.6, -0.4]$. Points in the grid: 1440 × 1440. The domain magnified in figure 3 is shown.

Figure 3.

Magnification of figure 2. Domain of x for Γ_- : $Re\, x \in (-10+0.88, -10+0.92]$, $Im\, x \in (-0.53, -0.49]$. Points in the grid: 1440 × 1440. The domain magnified in figure 4 is shown.

Figure 4.

Magnification of figure 3. Domain of x for Γ_- : $Re\, x \in (-10 + 0.90125, -10 + 0.90225]$, $Im\, x \in (-0.520, -0.519]$. Points in the grid: 1440 × 1440. The upper side of the domain magnified in figure 5 is shown.

Figure 5.

Magnification of figure 3. Domain of x for Γ_- : $Re\, x \in (-10 + 0.90145, -10 + 0.90170]$, $Im\, x \in (-0.52025, -0.520]$. Points in the grid: 1440 × 1440. The domains magnified in figures 6 and 7 are shown.

Figure 6.

Magnification of figure 5. Domain of x for Γ_- : $Re\, x \in (-10 + 0.9014625, -10 + 0.9015125]$, $Im\, x \in (-0.520225, -0.520175]$. Points in the grid: 1440 × 1440.

Figure 7.

Magnification of figure 5. Domain of x for Γ_- : $Re\, x \in (-10 + 0.9016, -10 + 0.90165]$, $Im\, x \in (-0.52005, -0.52]$. Points in the grid: 1440 × 1440. The domains magnified in figures 8 and 9 are shown.

Figure 8.

Magnification of figure 7. Domain of x for Γ_- : $Re\, x \in (-10 + 0.90162375, -10 + 0.90163375]$, $Im\, x \in (-0.520035, -0.520025]$. Points in the grid: 1440 × 1440.

Figure 9.

Magnification of figure 7. Domain of x for Γ_- : $Re\, x \in (-10 + 0.9016075, -10 + 0.9016125]$, $Im\, x \in (-0.5200125, -0.5200075]$. Points in the grid: 1440 × 1440.

Figure 10.

Magnification of figura 1. Domain of x for Γ_- : $Re\, x \in (-10+0.7475, -10+0.75]$, $Im\, x \in (-3.5, -2.5]$. Points in the grid: 480 × 1440.

Figure 11.

Wild set for the SM with $\epsilon = 0.5$. Order of the expansion (2.4): $n_0 = 50$. Cutting criterion : $M = 700$. Scale factor : $\mu = 0.25$. Maximun number of iterates : $N = 20000$. Domain D : $(0, 1] \times (0, 1]$. Number of jumps : $j = 0$. Points on the grid: 1440 × 1440.

Figure 12.

Same as figure 11 but with $j = 1$.

Figure 13.
Magnification of figure 11 around the secondary real homoclinic by a factor of 100.
Range in D : $(0.409, 0.419] \times (0, 0.01]$. Points in the grid: 1440 × 1440.

Figure 14.
Magnification of figure 11 around the secondary real homoclinic by a factor of 10000.
Range in D : $(0.4140675, 0.4141675] \times (0, 0.0001]$. Points in the grid: 1440 × 1440.

Figure 15.
Same as figure 12 but for $\epsilon = 0.1$.

Figure 16.
Magnification of figure 15 around the primary real homoclinic by a factor of 10000.
Range in D : $(0.3626925, 0.3627925] \times (0, 0.0001]$. Points in the grid: 1440 × 1440.

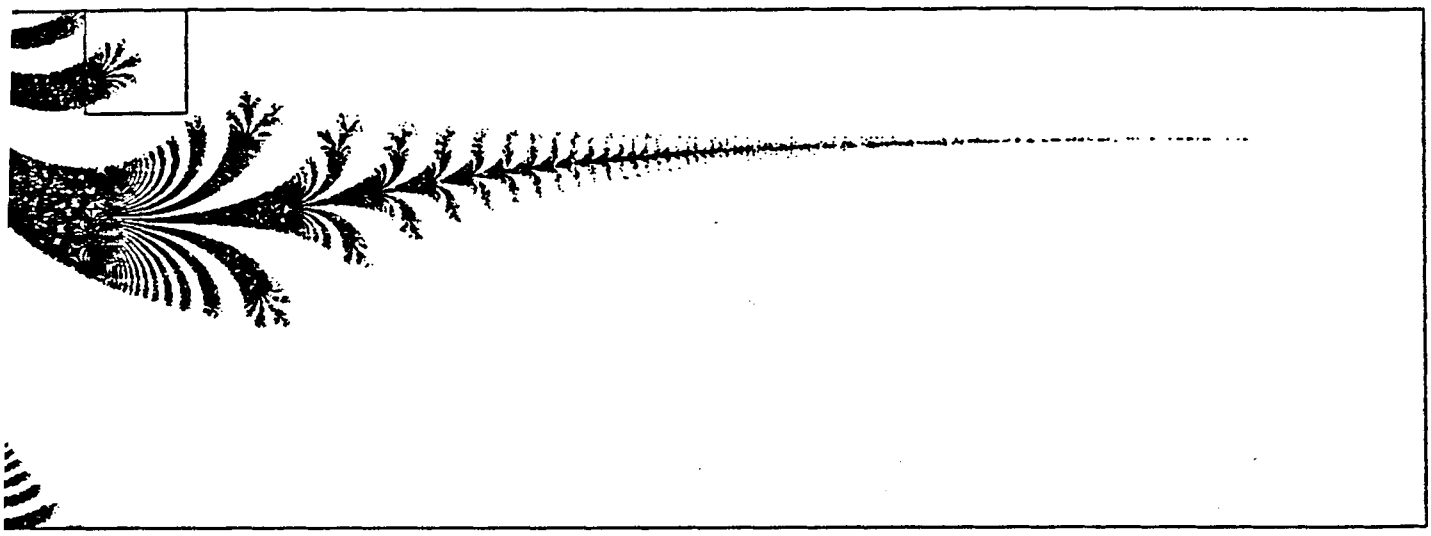

Fig. 1

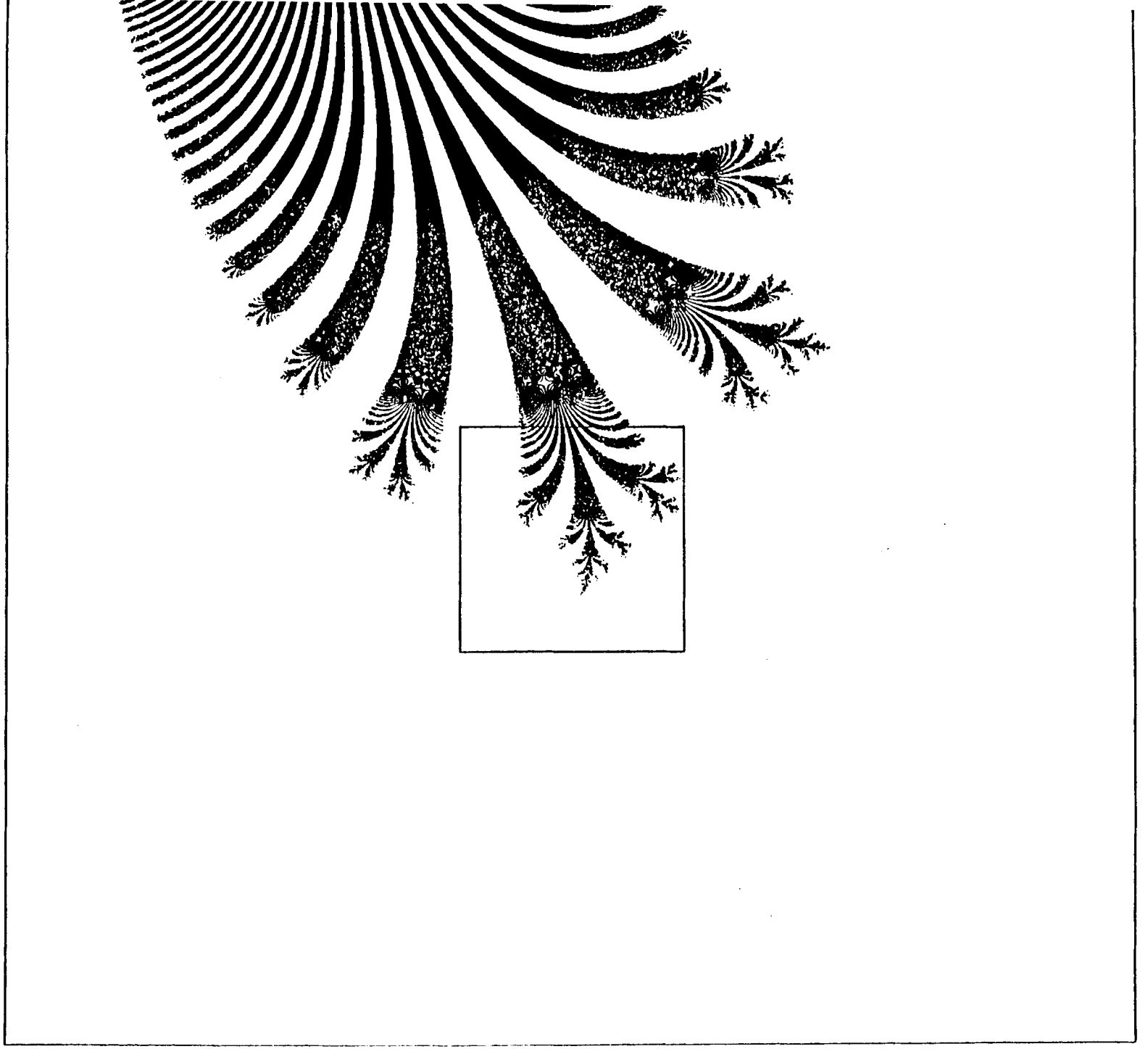

Fig.2

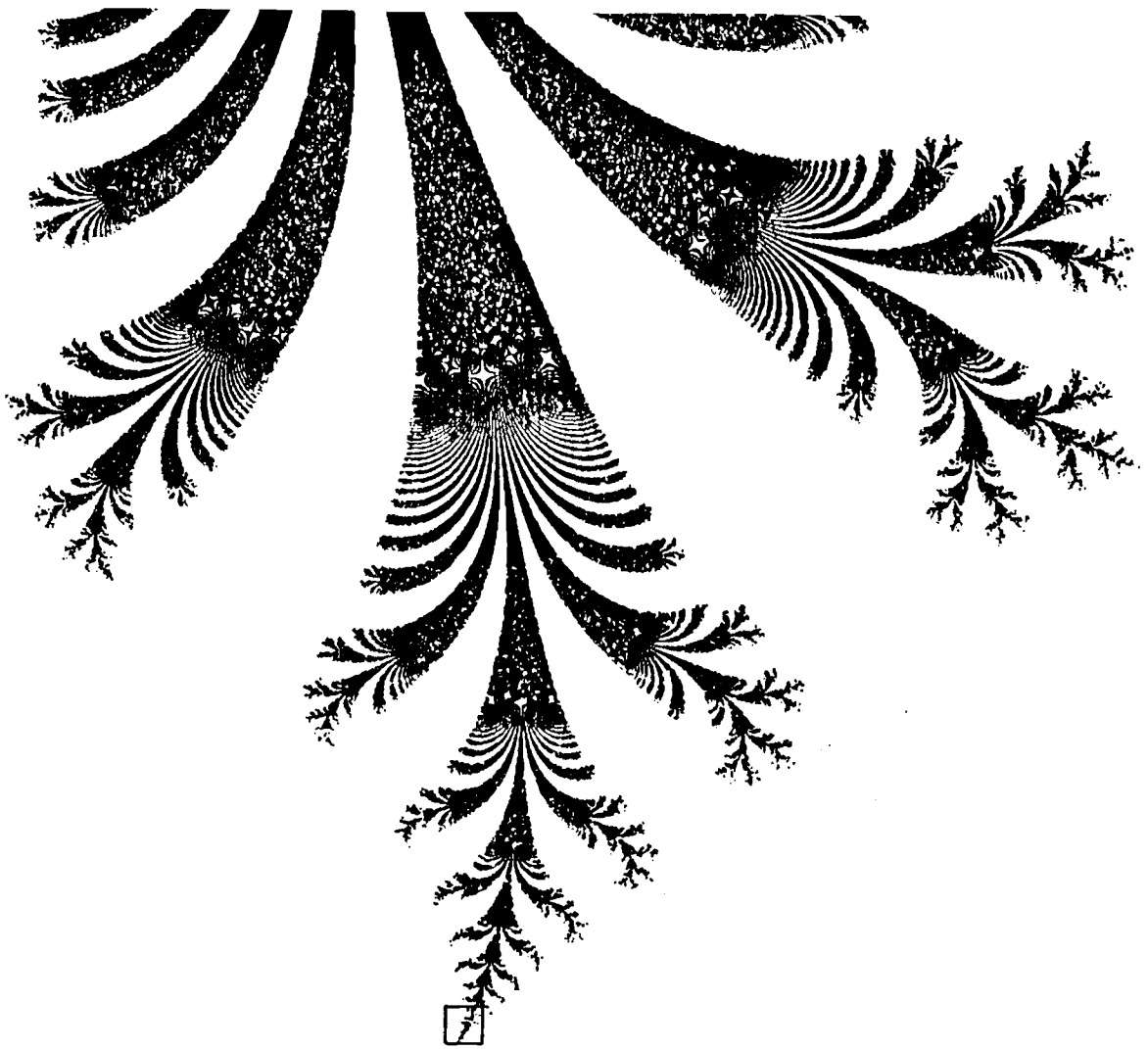

Fig.3

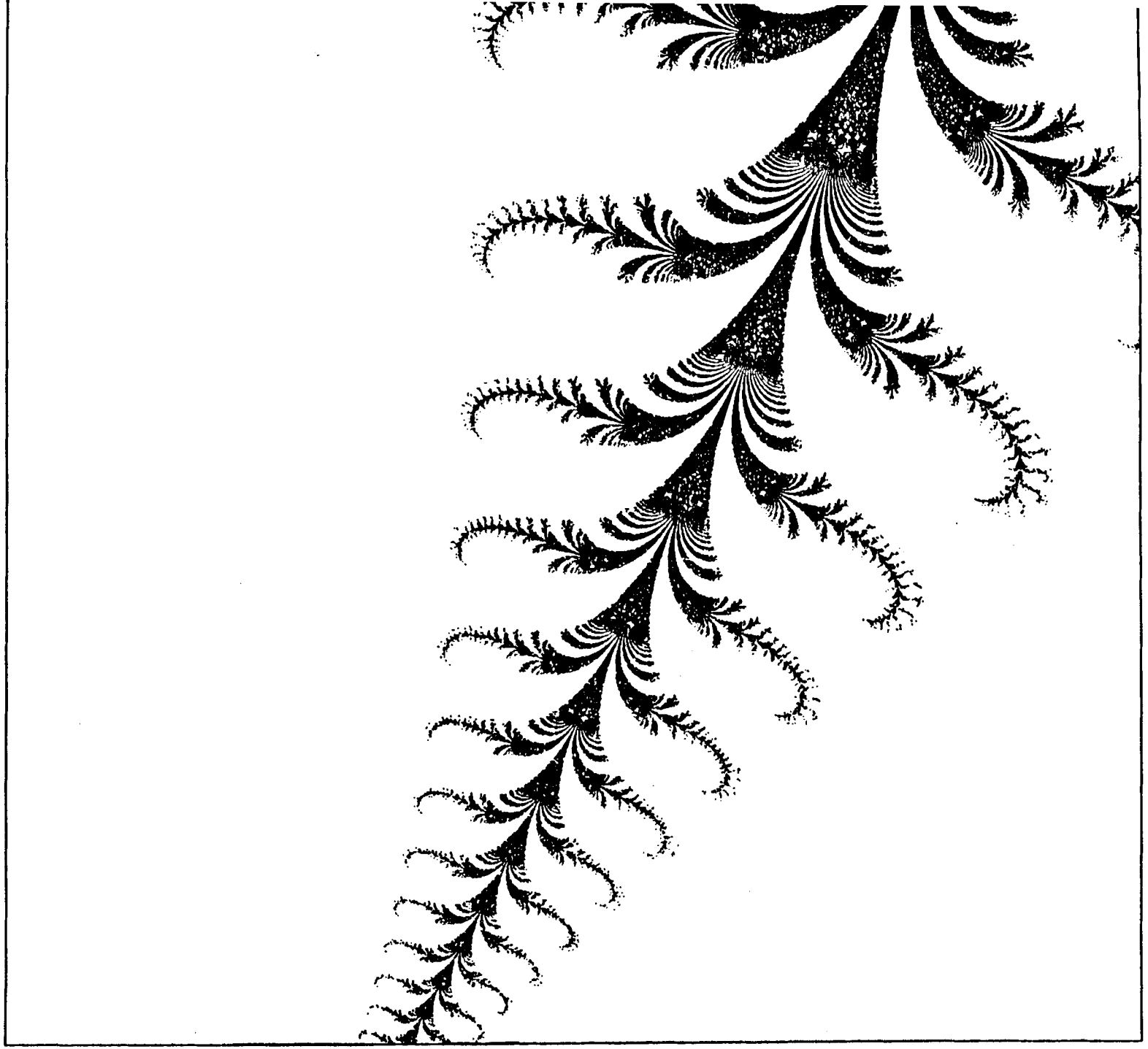

Fig. 4

Fig. 5

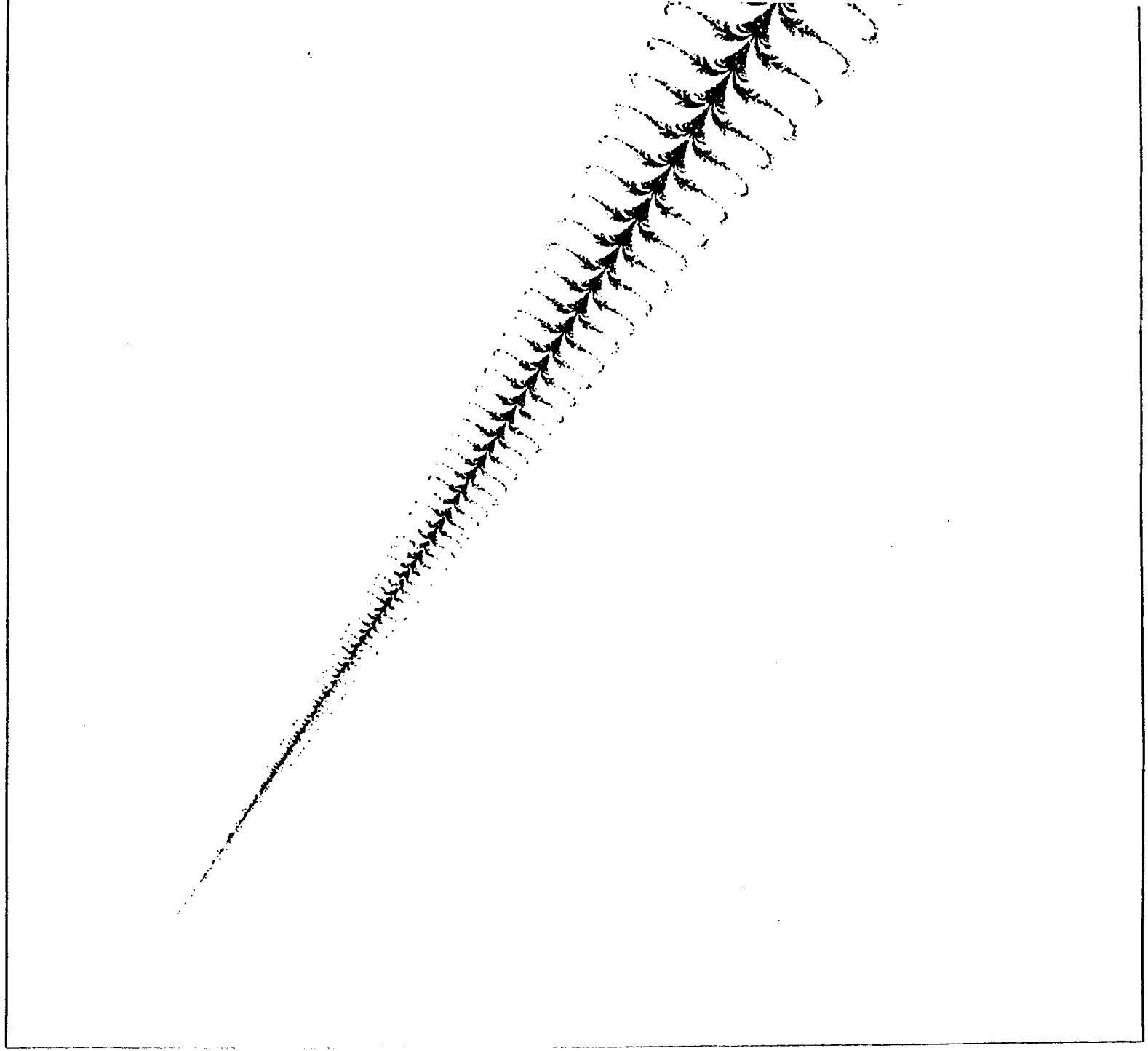

Fig. 6

Fig. 7

Fig. 8

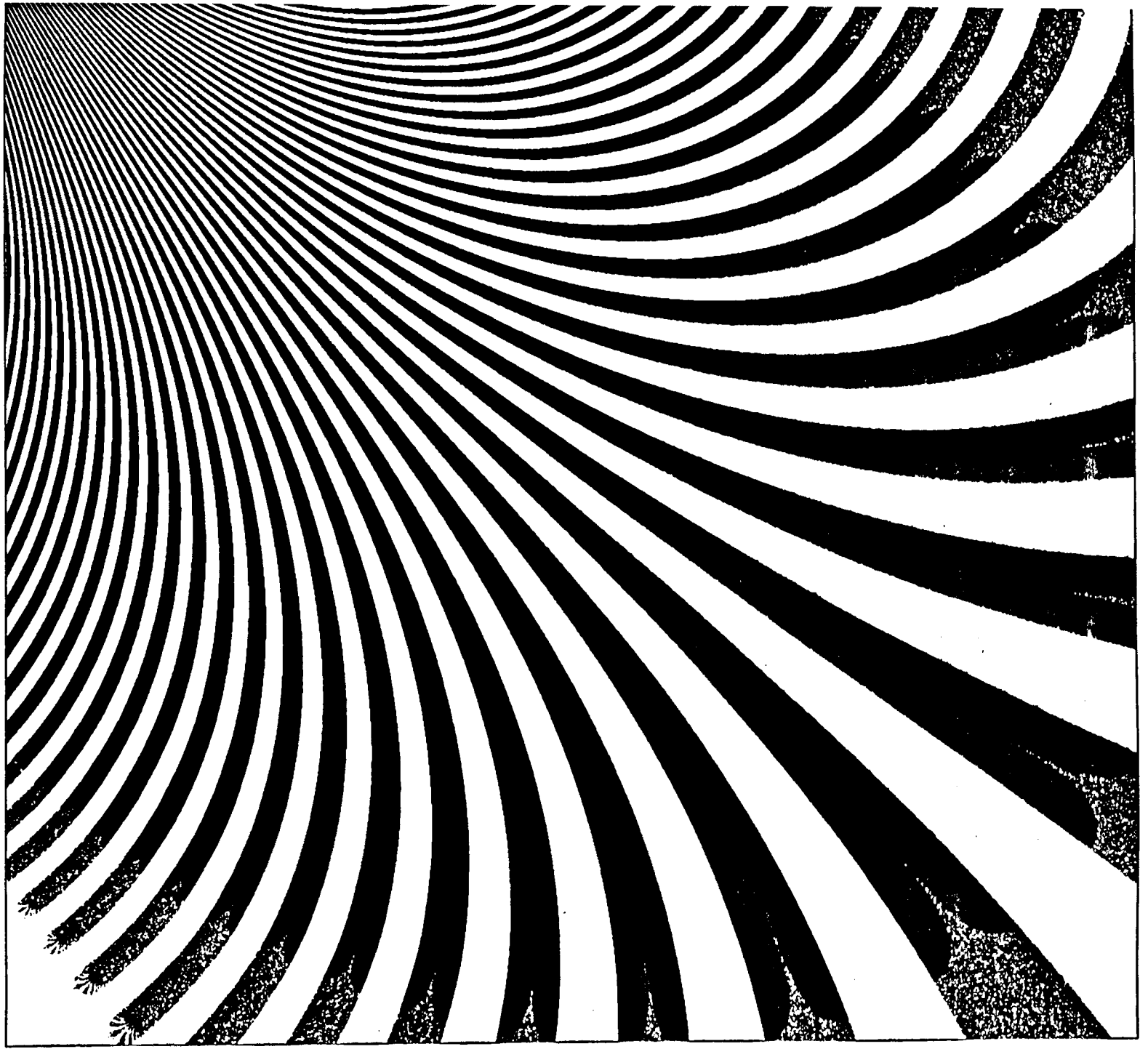

Fig. 9

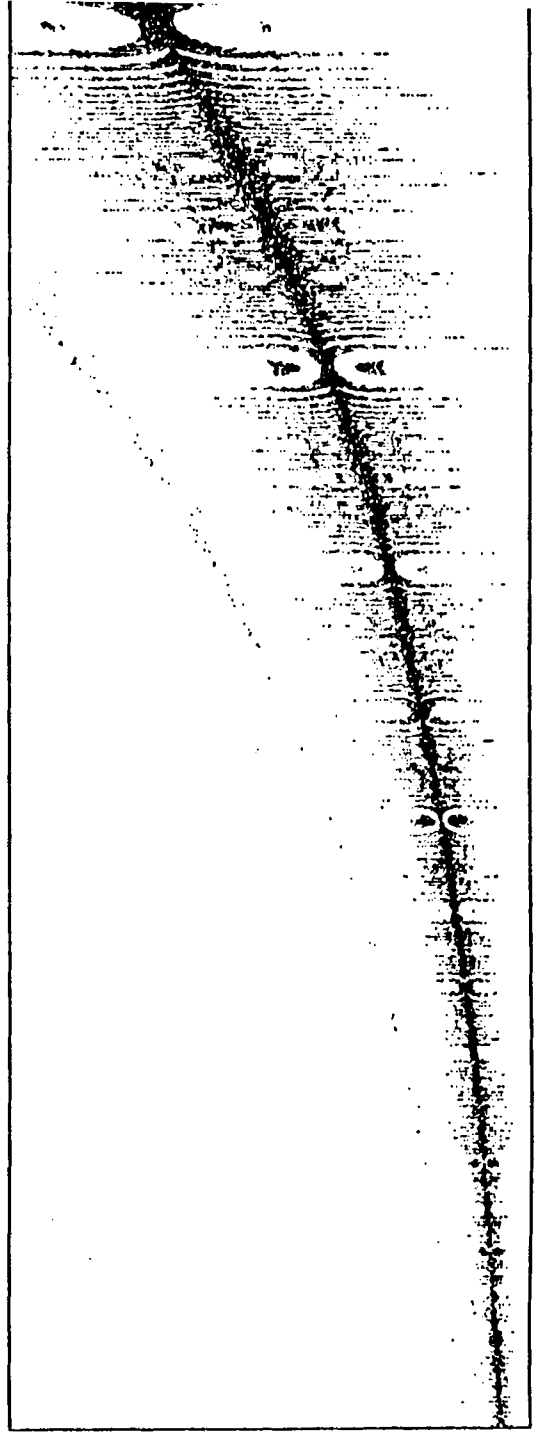

Fig. 10

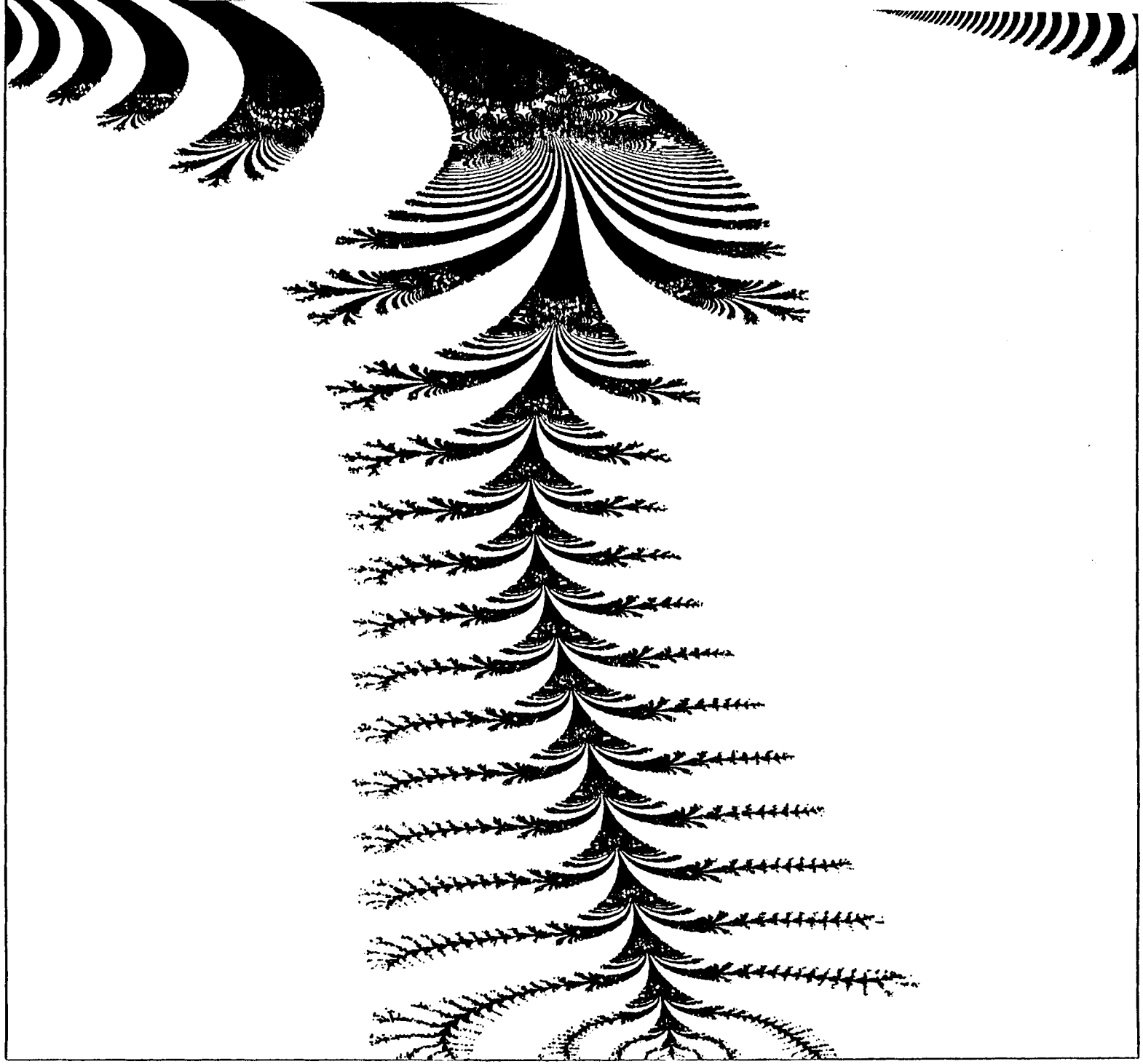

Fig. 11

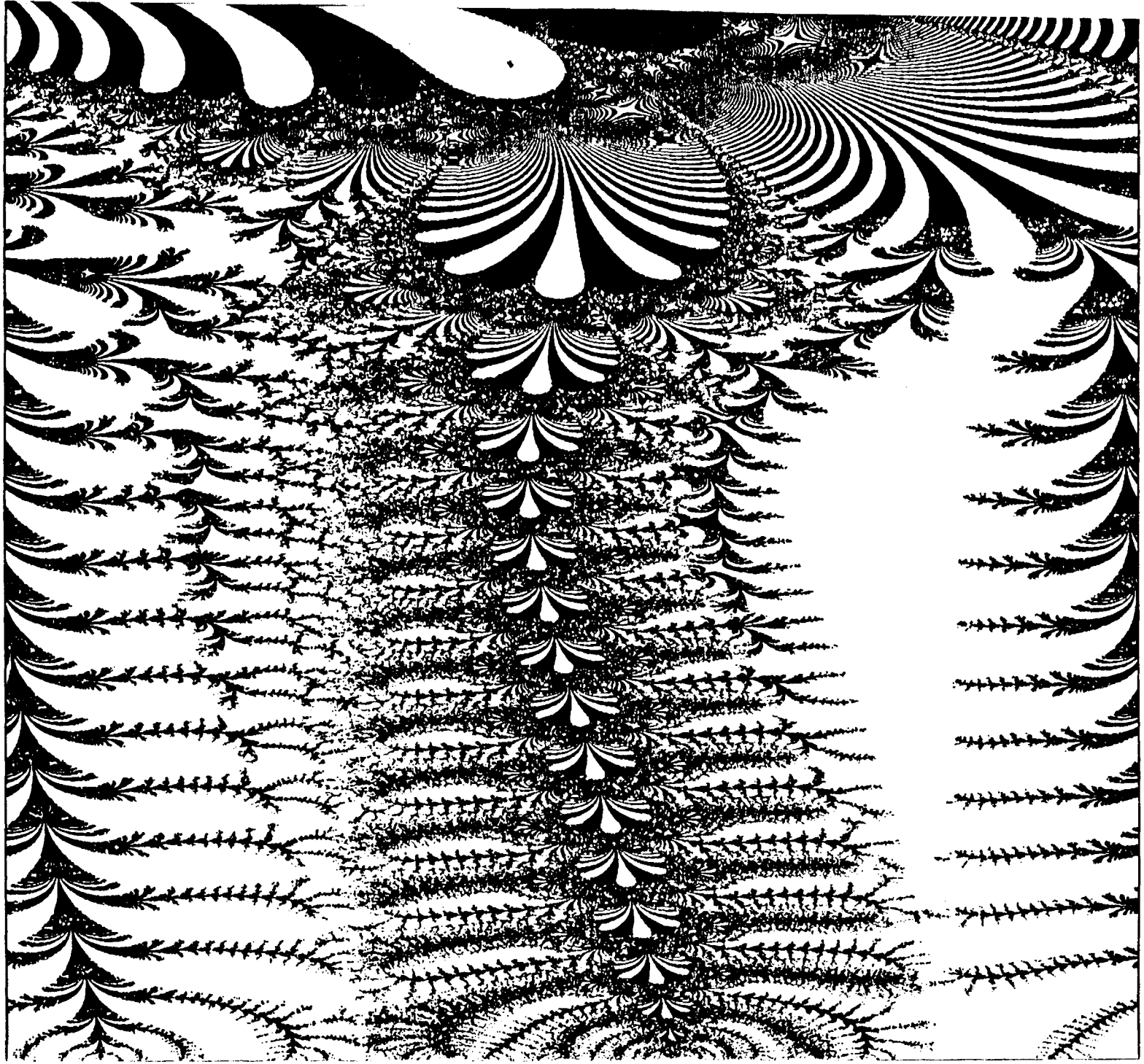

Fig. 12

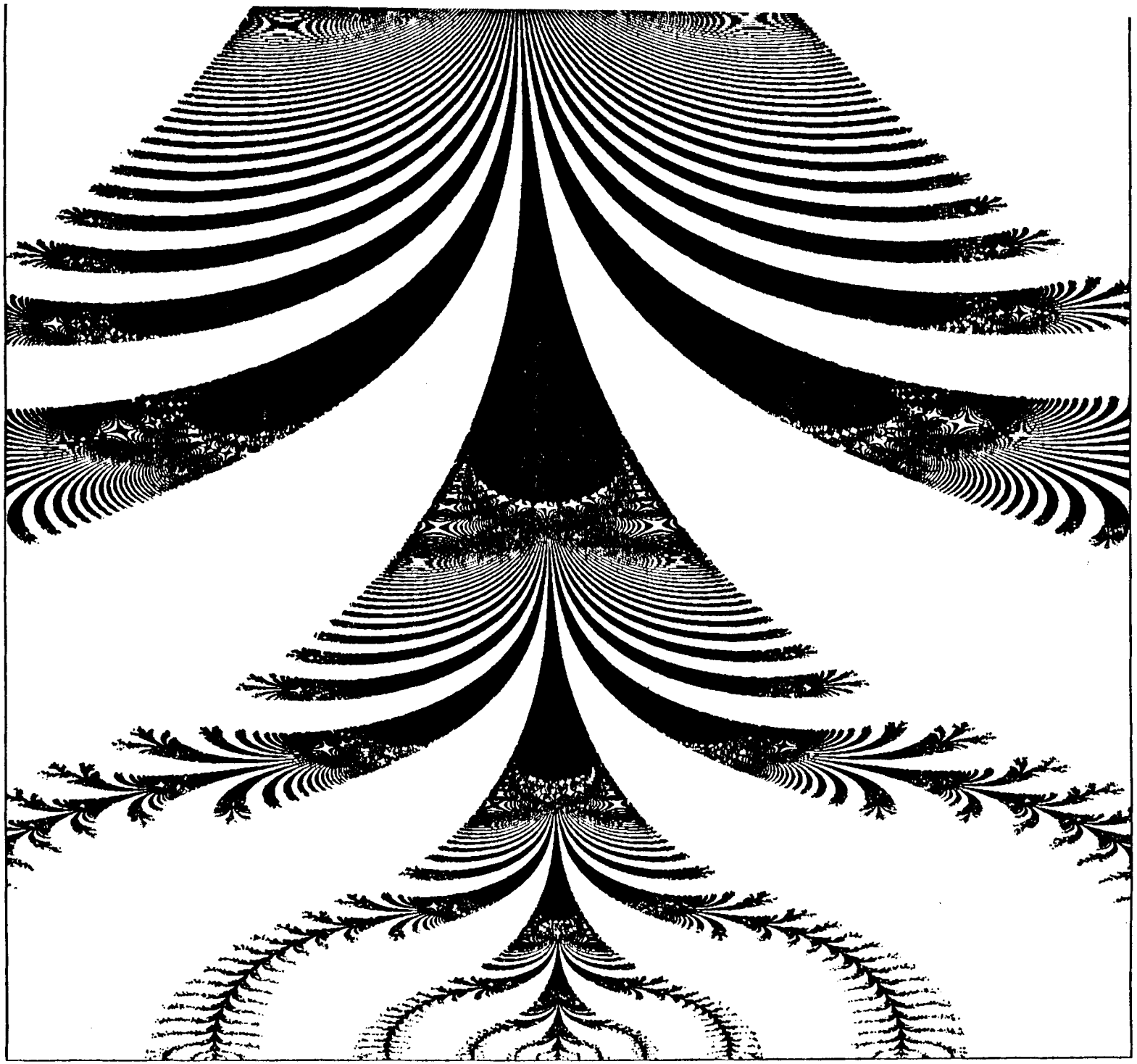

Fig. 13

Fig. 14

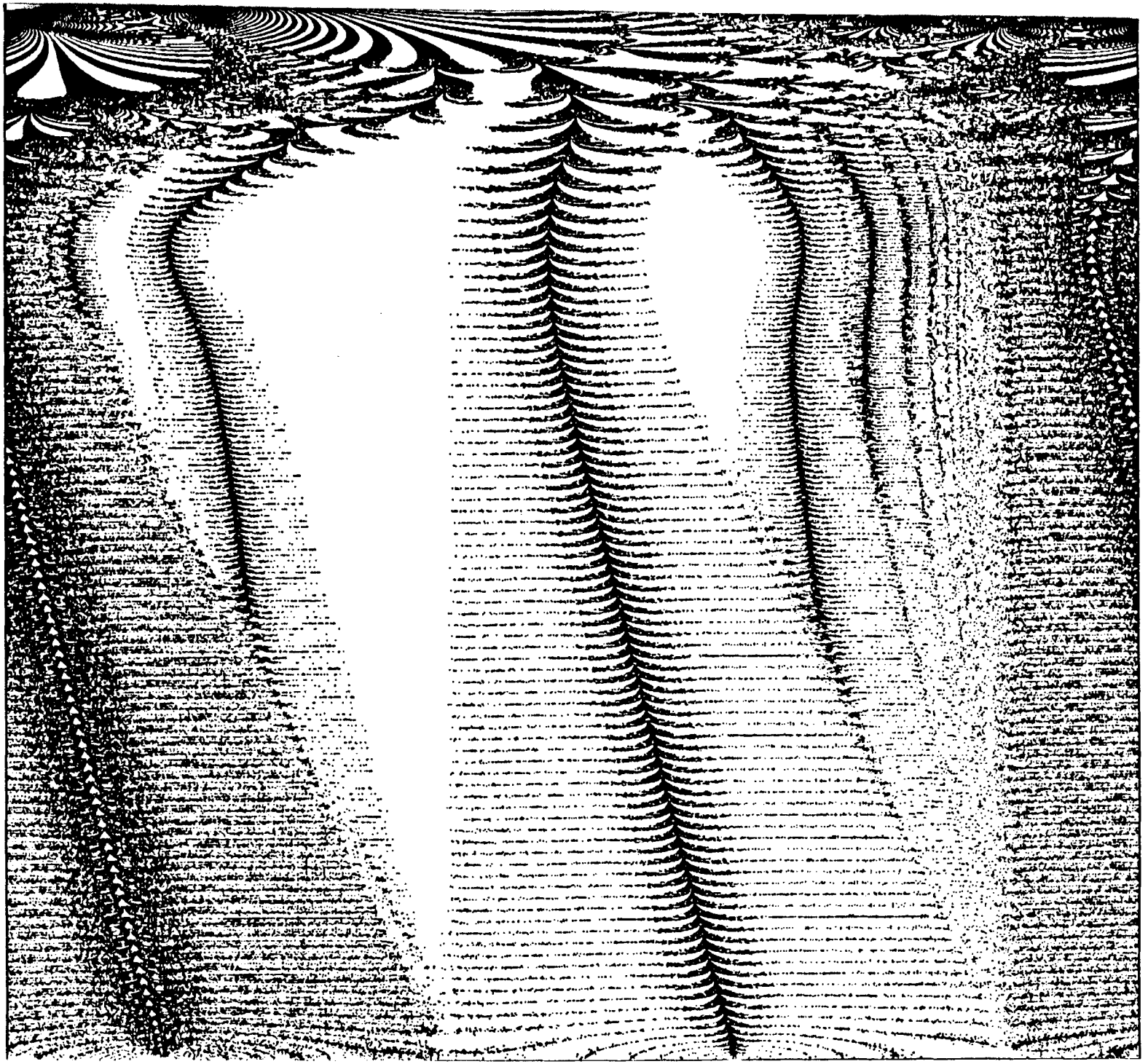

Fig. 15

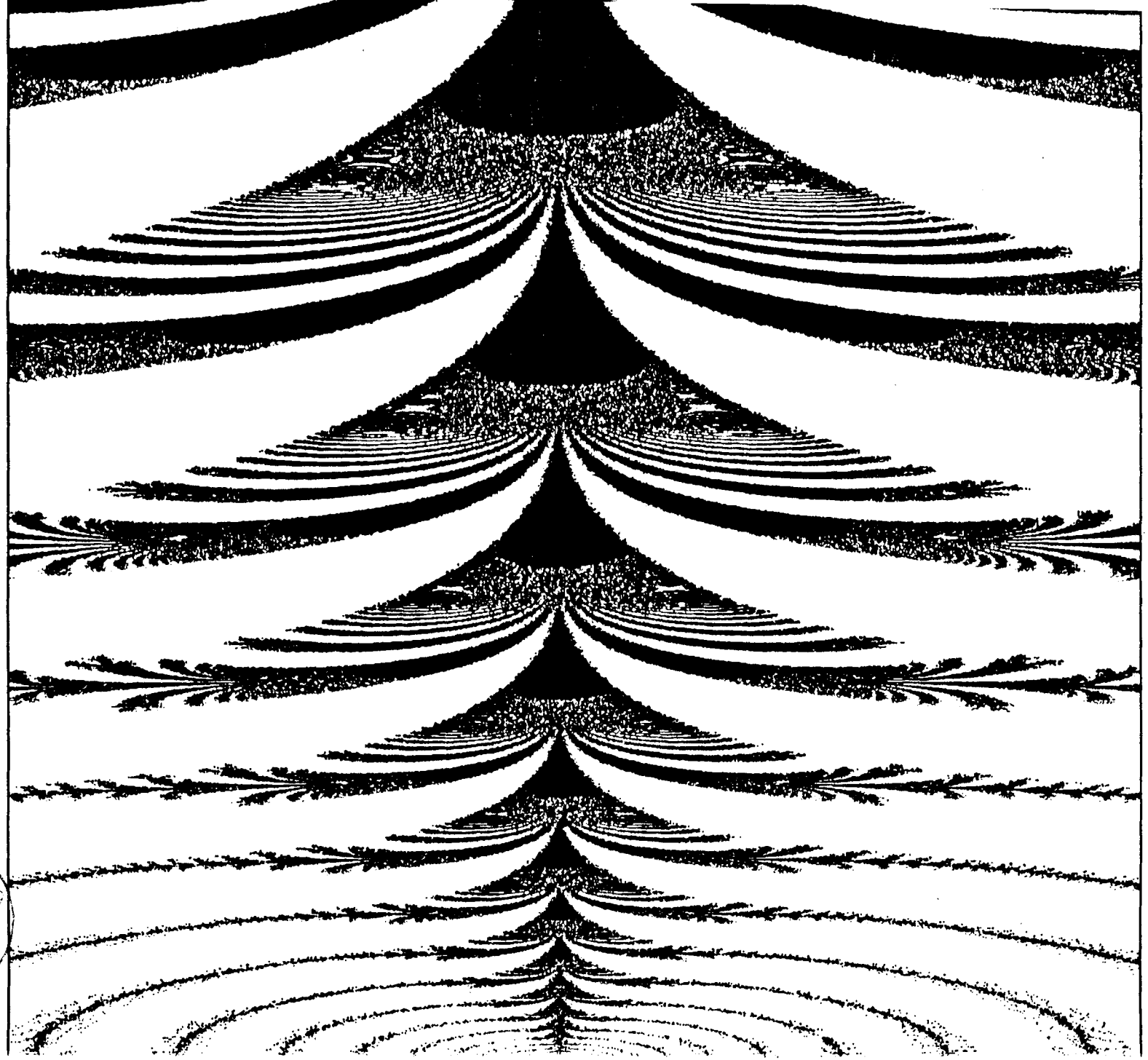

Fig. 16